



## Structural state of diamond-like amorphous carbon films, obtained by laser evaporation of carbon target

V.A. Plotnikov<sup>a,b,\*</sup>, B.F. Dem'yanov<sup>a</sup>, A.P. Yeliseyev<sup>c,d</sup>, S.V. Makarov<sup>a</sup>, A.I. Zyryanova<sup>a</sup>

<sup>a</sup> Altai State University, 61 Lenin av., 656049 Barnaul, Russian Federation

<sup>b</sup> Institute of Strength Physics and Materials Science SB RAS, 2 Akamicheskoy av., 634021 Tomsk, Russian Federation

<sup>c</sup> Institute of Geology and Mineralogy SB RAS, 3 Academician Koptyug ave., 630090 Novosibirsk, Russian Federation

<sup>d</sup> Novosibirsk State University, 2 Pirogova str., 630090 Novosibirsk, Russian Federation

### ARTICLE INFO

#### Keywords:

Amorphous carbon  
Pulsed laser deposition  
Vibrational properties characterization  
Microstructure  
Nanotechnology

### ABSTRACT

A homogeneous diamond-like film was obtained on an area of  $75 \times 25 \text{ mm}^2$ . Study of the film structure, using transmission electron microscopy and Raman spectroscopy, showed a mixture of carbon atoms with  $\text{sp}^2$ - and  $\text{sp}^3$ -bonds. Structure of carbon film is determined by the presence of randomly oriented carbon clusters bound by diamond  $\text{sp}^3$ -bonds (tetrahedral amorphous carbon, ta-C). Electron diffraction patterns demonstrate strongly distorted interfacial distances. Raman spectra show that there are carbon atoms with graphite  $\text{sp}^2$ -bonds in the film, but a signal of graphite crystal lattice is absent in electron diffraction: This implies that hexagonal units are not shaped into a graphite crystal lattice. Broad D-band in Raman spectra shows strongly distorted carbon bonds in graphite. If diamond phase dominates, the space between diamond clusters is filled with carbon atoms with  $\text{sp}^2$ -bonds (turbostratic structure). Thus, diamond areas are bound into a single discontinuous aggregate of carbon diamond-like film.

### 1. Introduction

The properties of carbon films are determined by a large diversity of structures which have not only crystalline, but also amorphous state. This diversity of structures and the unique properties of diamond films can be explained by the features of interatomic bonds between carbon atoms. The most widespread chemical bonds in amorphous and crystalline carbon films are the  $\text{sp}^3$ - and  $\text{sp}^2$ -bonds which are a result of electronic orbitals hybridization. At  $\text{sp}^3$ -hybridization carbon atoms have four  $\text{sp}^3$ -orbitals, which allows them to form four strong bonds with the neighboring atoms. In some carbon films, the portion of  $\text{sp}^3$ -bonds reaches 80% and more [1–3], which results in their high hardness. Such films consist of tetrahedral amorphous carbon, in which diamond  $\text{sp}^3$ -bonds dominate [1,2,4,5]. In  $\text{sp}^2$  configuration carbon bonds form three  $\text{sp}^2$  orbitals (three strong covalent bonds) and a weak  $\pi$ -bond (Fig. 1b), and the structure consists of flat rings which are joined into the graphite phase with the help of  $\pi$ -bond [6].

To describe the structure of amorphous films, the cluster model was suggested [7,8]. The substance of this model is as follows. Carbon atoms tied by  $\text{sp}^2$  bonds are joined into plates consisting of rings. These rings are joined by  $\pi$ -bonds into stacks and form graphite clusters. These clusters are buried into the matrix of carbon atoms bound by  $\text{sp}^3$ -bonds.

The  $\text{sp}^2$ -clusters determine the electrical properties whereas  $\text{sp}^3$ -matrix controls the mechanical properties. The heterogeneity of film structure follows from this model: the areas with  $\text{sp}^2$  and  $\text{sp}^3$  bonds are alternating here.

Thus, in amorphous and nanocrystalline carbon films the areas with coordination numbers 3 ( $\text{sp}^2$ -bond) and 4 ( $\text{sp}^3$ -bond) may exist: they form a mixture of structures with different types of bonds [7]. At first, the high hardness was considered to be determined by diamond  $\text{sp}^3$ -bond, but recent studies showed that  $\text{sp}^2$ -bonds also form carbon films of high hardness. This means that the existence of this or the other bond does not attest to the predominance of properties typical of diamond or graphite, provided that  $\text{sp}^2$  and  $\text{sp}^3$  clusters are nanosized [9,10].

Amorphous state in materials with covalent bonds differs considerably from amorphous state in metals. Amorphous metals have a liquid-like structure, in which the nearest environment of atom follows the principle of the closest packing, the neighbors being located at a distance of atomic diameter to each other, whereas coordination number is close to 12. In covalent crystals the distance to the nearest neighbors is determined by the length of covalent bond, whereas the number of nearest atoms is determined by the element valency. In diamonds, the nearest atoms are located at a distance of 0.154 nm, number of nearest neighbors is 4. In graphite, these parameters are

\* Corresponding author at: Altai State University, 61 Lenin av., 656049 Barnaul, Russian Federation.

E-mail address: [plotnikov@phys.asu.ru](mailto:plotnikov@phys.asu.ru) (V.A. Plotnikov).

<https://doi.org/10.1016/j.diamond.2018.11.022>

Received 24 August 2018; Received in revised form 24 October 2018; Accepted 21 November 2018

Available online 22 November 2018

0925-9635/© 2018 Published by Elsevier B.V.



**Fig. 1.** A diamond-like amorphous carbon film deposited on the silicate glass substrate obtained by laser evaporation of carbon target. The dimension of the area covered with film is  $75 \times 25 \text{ mm}^2$ .

0.142 nm and 3, respectively.

In this paper, we have carried out the investigation of the structure of a thin carbon film obtained by laser evaporation of carbon targets in vacuum.

## 2. Experimental

Structure of carbon films depends on the regime of carbon atom condensation on the substrate. Varying this regime, one can control the film properties in a broad range. Laser evaporation produces mainly  $\text{sp}^3$ -bonds in condensed carbon, the so-called ta-C carbon [8]. We used direct evaporation of graphite target at 1064 nm laser irradiation from a Nd:YAG laser NTS300 to condense carbon on amorphous substrate of silicate glass. Defocused laser beam is introduced into the vacuum chamber of the vacuum unit (the residual pressure is less than  $10^{-5}$  Torr), where graphite targets and silicate glass substrates were placed. On a graphite target with a diameter of 5 mm and a thickness of about 2 mm, the defocused laser beam, whose energy was 1.1–1.9 J, created a spot with a diameter of about 3 mm. The exposure time was about 5 min. The resulting stream of evaporated carbon was deposited on glass substrates, which were arranged in a circle with a diameter of about 20 cm at a distance of about 10 cm from the target and at an angle of about  $30^\circ$  to the axis of the vapor-gas torch, forming a carbon film. If the target is heated by a defocused beam, target fragmentation is absent. The resulting diamond-like amorphous carbon film is shown in Fig. 1. Carbon condensation from the vapor phase was carried out on the silicate glass substrate  $75 \times 25 \text{ mm}^2$  in size. Detonation ultrananocrystalline diamonds, studied for comparison, were produced according to technical specifications TU 84-112-87 in the Federal Research and Production Center “Altai”, Biysk, Russia.

Structural studies were carried out on a transmission electron microscope Philips CM-30 in the Material science center of collective usage at Tomsk State University. Raman spectra were recorded at room temperature using a micro-Raman LabRAM HR spectrometer with 325 nm excitation from a He-Cd laser (IGM SB RAS).

## 3. Results

### 3.1. Transmission electron microscopy of thin carbon film

The structure of thin carbon film was studied using transmission electron microscopy (TEM). A typical section of such film is shown in Fig. 2a with magnification which is sufficient to reveal details smaller than 1  $\mu\text{m}$ . Film structure is a homogeneous matrix the main feature of which is the absence of any boundaries. Some contrast observed in the bright-field TEM image is due to variations in the film thickness, i.e., to the weak relief on the film surface.

To determine the structural state of the carbon film, the electron-diffraction patterns were obtained for several sections. The image of carbon film and corresponding electron-diffraction (ED) pattern are given in Fig. 1. Analysis of such patterns showed that the rings

(diffraction maxima) correspond to the diffraction from (111) and (220) faces of diamond lattice. Interfacial distances are  $d_{111} = 0.207 \text{ nm}$  and  $d_{220} = 0.119 \text{ nm}$ . One can see that these values differ from the table values for diamond ( $d_{111} = 0.205 \text{ nm}$  and  $d_{220} = 0.125 \text{ nm}$ ). For the film, the interfacial distance  $d_{111}$  is larger whereas distance  $d_{220}$  is smaller in comparison with the values for a diamond single crystal. Such distortion of the lattice is typical of thin diamond-like films. For example, in [11], thin carbon films obtained by laser evaporation and carbon condensation were studied and values of interfacial distances  $d_{111} = 0.208 \text{ nm}$  and  $d_{220} = 0.117 \text{ nm}$  were given. The authors of [12] obtained  $d_{111} = 0.207 \text{ nm}$ . One can suppose that interfacial distances do not change and the length of the C–C bond remains permanent but the angles between bonds vary similar to carbon nanotubes and fullerenes [13,14]. This results in lattice distortion with a decrease in some interfacial distances and with an increase in the others.

Strong broadening of the rings is an important feature of the ED pattern. If the size of diamond crystals is 4 to 7 nm, then broadened but rather well-pronounced diffraction reflections are observed [15,16]. Thus, it is possible to suppose that the size of areas forming the diffraction ring is considerably smaller, supposedly about 1 nm. Similar broadening of the rings in the ED pattern for a diamond-like film was described in [3]: This was due to 80% of the  $\text{sp}^3$ -bonds. Such structure corresponds to ta-C amorphous diamond [17]. Thus, amorphous carbon can be considered to be a mixture of  $\text{sp}^2$ - and  $\text{sp}^3$ -bonds [18].

The situation with carbon materials with strong covalent bonds is much more complicated. It is impossible to interpret the amorphous state as the liquid-like state in covalent crystals. If the closest neighbors are located at a distance from the first coordination sphere as in the case of metallic amorphous materials, then coordination number will be determined by the bond type ( $\text{sp}^2$  or  $\text{sp}^3$ ). However, in any case the principle of the closest packing is not realized in carbon amorphous materials. Amorphous carbon material is characterized, first of all, by the random chaotic combination of interatomic  $\text{sp}^2$ - and  $\text{sp}^3$ -bonds.

Electron microscopy and electron diffraction allow us to unambiguously interpret the structural state of the carbon film as diamond-like. But highly diffused reflexes indicate extremely small size of diamond clusters and strong distortion of interatomic distances. According to publications such ED pattern determines that the structural state of the carbon film is amorphous, so-called ta-C (tetrahedral amorphous carbon) [19]. However, the relative position of the rings clearly indicates some crystallinity in the diamond component of the film. On the other hand, no reflexes from the hexagonal crystal lattice of graphite were found. The question arises whether there is carbon with  $\text{sp}^2$ -bonds in the structure of such film. The answer is given by the Raman spectroscopy.

### 3.2. Raman spectroscopy of thin diamond-like films

Raman spectra were recorded in 14 points, distributed evenly, with an interval of 0.5 cm, along a line parallel to the long edge of the substrate. These Raman spectra were found to be very similar and one of them is given in Fig. 3. Main features of Raman spectrum are two broad bands near  $1393$  and  $1607 \text{ cm}^{-1}$ . A band at larger wave number is attributed to the optical stretching mode of  $E_{2g}$  symmetry (G-mode). This band is located at  $1585 \text{ cm}^{-1}$  in well-ordered, perfect crystalline graphite, but it is shifted to  $1607 \text{ cm}^{-1}$  in our case because of the graphite disordering [19]. For natural crystalline graphite, this band is narrow and the full width at half-maximum (FWHM) is about  $13 \text{ cm}^{-1}$ . Broadening to  $80 \text{ cm}^{-1}$  is commonly explained by the presence of glass-like graphite. Line near  $1355 \text{ cm}^{-1}$  is D-mode or a disorder peak. Tuinstra & Koenig attributed to the breathing mode of  $A_{1g}$  symmetry with phonons corresponding to the point  $k = 0$  [20]. This mode is absent in perfect graphite and appears only at its disorder. Its position varies in the  $1310$  to  $1450 \text{ cm}^{-1}$  range whereas FWHM values cover the  $80$  to  $400 \text{ cm}^{-1}$  range. A possible origin is disordered or nanocrystalline graphite, disordered glass-like carbon,  $\text{sp}^2$ -hybridized carbon phases

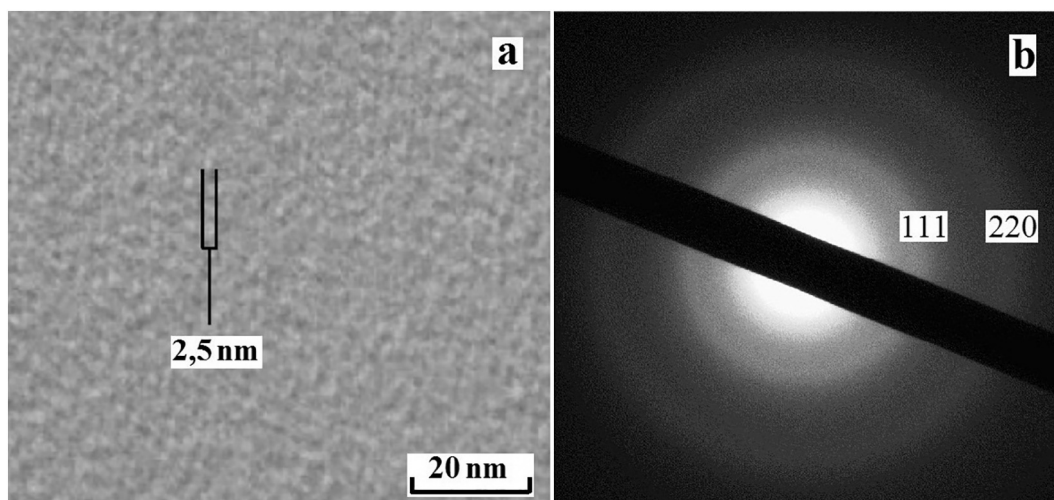


Fig. 2. Bright-light TEM image of carbon film (a) and electron-diffraction pattern for the same area (b).

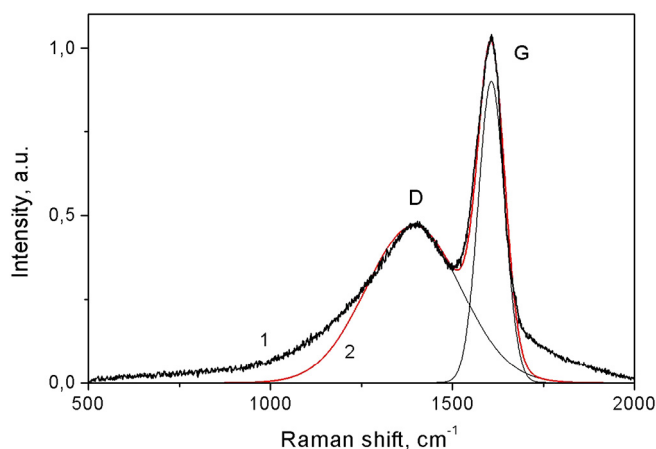


Fig. 3. Raman spectrum for point 6 on diamond-like carbon film (1) and results of its decomposition into two Gaussian components with maxima near 1393 and 1607  $\text{cm}^{-1}$  and FWHM values 300 and 88  $\text{cm}^{-1}$ , respectively. Curve 2 is a sum of two Gaussian components whereas thin black lines show individual components. For given point 6 the ratio  $I_D/I_G$  is about 0.53.

or microcrystalline defect graphite [21]. The intensity of D peak changes depending on the number of aromatic rings in the graphite-like clusters. Although Raman spectra are not a measure of the  $\text{sp}^2$ - or  $\text{sp}^3$ -input, some parameters of these spectra (for example, position of G-peak or the  $I_D/I_G$  ratio) provide such information. Thus, the shift of G-peak to high energies and increase in the  $I_D/I_G$  value indicate an increase in  $\text{sp}^2$   $\pi$ - $\pi^*$  bonding or, per contra, a decrease in diamond-like  $\text{sp}^3$  bonding [18].

Decomposition into two, D and G, components was carried out for all 14 Raman spectra, recorded in different points. The dependences of the intensities of the peaks D and G, as well as of the ratio  $I_D/I_G$  between these two values on the coordinates of the measurement points distributed uniformly along the substrate about 7.5 cm long are shown in Fig. 4a. In Fig. 4b similar dependencies are shown for the width of these peaks. It can be seen that the latter are virtually independent of the coordinates. As for the intensities of the bands D and G, they gradually increase (by 25–35% from left to right on the film in Fig. 1) and further in the last two points fall to the initial level. The  $I_D/I_G$  ratio in the same range varies from 0.48 to 0.58.

#### 4. Discussion

According to the results of electron microscopy, a typical structural

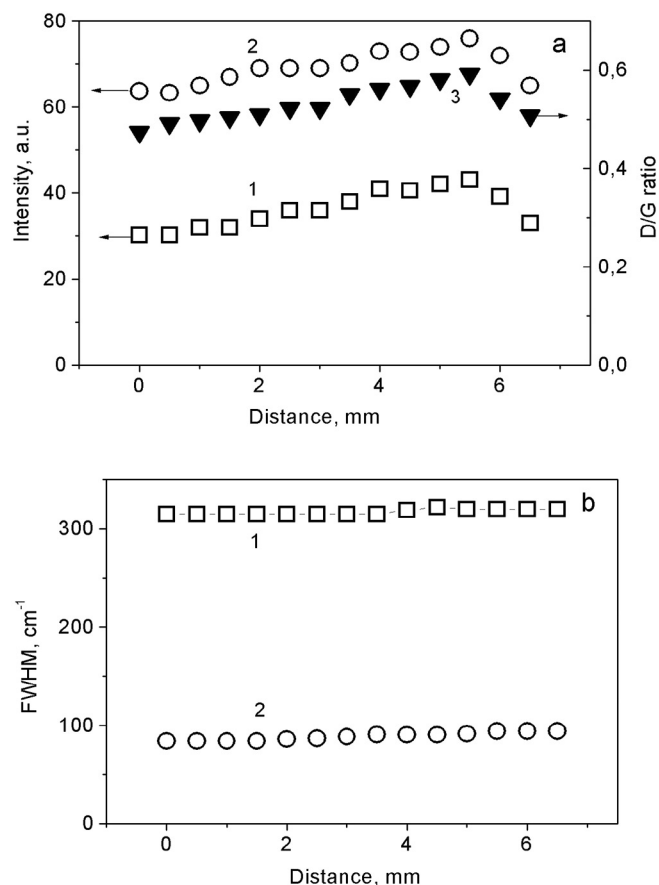


Fig. 4. Parameters of Raman spectra recorded in 14 points of the diamond-like carbon film (see Fig. 1):

- (a) Intensities of Gauss components D (1) and G (2), and  $I_D/I_G$  ratio (3) versus coordinate;  
 (b) FWHM values for D and G peaks versus coordinate (1 and 2, respectively).

feature of thin carbon film is the absence of well-pronounced boundaries between grains, which attests to the amorphous state. However, electron-diffraction patterns show unambiguously the presence of a diamond crystal lattice, though it has changed interfacial distances. Graphite reflections are absent in these patterns.

On the contrary, analysis of Raman spectra attests to the presence of both the D line of disordered graphite and the G line of perfect

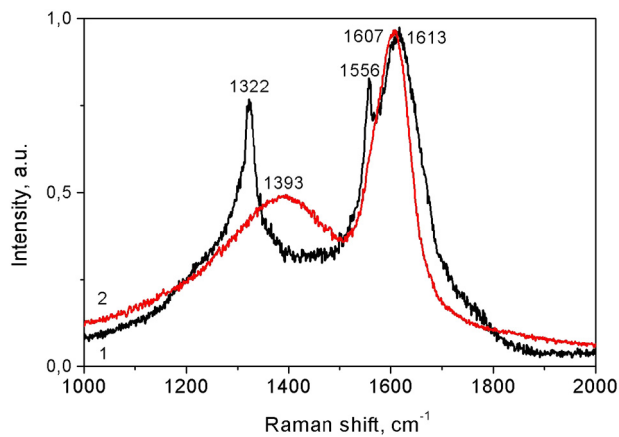


Fig. 5. Raman spectrum for detonation nanodiamond (1) and carbon diamond-like film (2).

crystalline graphite. The results of these two techniques used for studying the structure state of diamond-like films seem to contradict one another. However, this contradictory situation is solvable. The high symmetry of diamond lattice is known to determine the simplicity of vibrational spectrum. There is a single triply degenerated fundamental vibration which is located at  $1332.5 \pm 0.5 \text{ cm}^{-1}$  at room temperature in a perfect diamond lattice [22]. In nanocrystalline diamond the FWHM value increases, but in tetragonal and amorphous films this peak is completely absent [22]. Indeed, in nanocrystals of detonation diamond a broadened  $1322 \text{ cm}^{-1}$  line is present (Fig. 5): it is superimposed on the broadband spectrum of graphite with main maxima near  $1317$  and  $1613 \text{ cm}^{-1}$  (D and G lines, respectively). The position of these maxima depends considerably on the  $\text{sp}^2$  configuration of carbon [19] and the size of graphite grains.

D peak with maximum in the  $1345\text{--}1358 \text{ cm}^{-1}$  range, corresponding to polycrystalline graphite, is typical of amorphous films of diamond-like carbon. The intensity of this peak decreases as the size of graphite grains grows. Simultaneously the peak broadens and shifts to higher energies. In our case D peak is abnormally broadened, covers the  $1000$  to  $1600 \text{ cm}^{-1}$  range and has a maximum near  $1393 \text{ cm}^{-1}$  (Figs. 3, 4). This may attest to the considerable distortion of bonds with  $\text{sp}^2$  hybridization. Diamond peak with the maximum at  $1322 \text{ cm}^{-1}$  is located just in this range.

In a number of papers the ratio between the intensities of D and G peaks was shown to be associated with the carbon portions in  $\text{sp}^2$  and  $\text{sp}^3$  hybridizations [23]. To obtain the  $L = I_D/I_G$  parameter, we decomposed the Raman spectrum into two Gaussian components (Fig. 4). Here  $I_D$  and  $I_G$  are the intensities of D and G components, respectively, and  $L$  is the characteristic coefficient showing the portion of carbon atoms with  $\text{sp}^2$  hybridization. For diamond-like films of amorphous carbon the  $L$  values do not exceed 0.6. In our case  $L$  varies in the 0.48 to 0.58 range.

The obtained results can be explained in a cluster model [7,8]. Cluster state affects considerably the appearance of electron-diffraction patterns for carbon diamond-like films. Such patterns (electronic reflections) are solid rings for a fine-grained polycrystal, with the width of the rings being broadened as the grain size decreases. These reflections remain pronounced until atoms form a crystal lattice in the samples. At a certain size crystals transform to clusters. A cluster is a group of atoms bound by interatomic interaction and crystal lattice is not surely formed in such group. Nanocrystal, 5 nm in size, contains about  $2 \times 10^4$  atoms, whereas there are about  $10^3$  atoms in a 1 nm nanocrystal. Such a small amount of atoms cannot provide diffraction on crystallographic planes and ring formation in the ED patterns. In our case the ED pattern indicates that diamond crystal structure is already formed. Reflections from the graphite component are absent. This allows us to suppose that

graphite platelets, consisting of hexagonal rings, are misoriented to each other and do not form a hexagonal lattice. This, so-called turbostratic structure [6,24] binds diamond areas into a single discontinuous aggregate of carbon film. Fig. 1a shows the cluster structure of the diamond-like film, according to which the size of the diamond cluster is about 2.5 nm.

Thus, the structural state of the film is as follows: basically, the structure of the film is diamond clusters united in a coherent homogeneous structure by carbon atoms but with  $\text{sp}^2$  bonds. This approach is an alternative to approach, according to which carbon clusters, bound by  $\text{sp}^2$ -bonds, are organized into planes, consisting of hexagonal rings. These rings are bound by  $\pi$ -bonds into stacks and form graphite clusters. These clusters are immersed in a matrix of carbon atoms bound by  $\text{sp}^3$ -bonds [8]. TEM of carbon thin films attests unambiguously, and Raman spectroscopy indirectly indicates the presence of diamond  $\text{sp}^3$ -bonds and the organization of carbon atoms in nanodiamond clusters. The abnormally broadened reflexes also indicate large distortions of interplanar distances  $d(111)$  and  $d(220)$ . The absence of graphite phase reflexes indicates the absence of pronounced graphite clusters. We can suppose that the structure of our film consists of diamond nanoclusters, where carbon atoms are bound by  $\text{sp}^3$  bonds, but the space between clusters is filled with carbon atoms with  $\text{sp}^2$ -bonds.

Electron microscopy of thin carbon films attests unambiguously and Raman spectroscopy attests indirectly to the presence of diamond  $\text{sp}^3$  bonds and to the configuration of carbon atoms into nanodiamond clusters, whereas the abnormally broadened reflections show strong distortions of interfacial distances  $d(111)$  and  $d(220)$ . Absence of graphite reflections indicates the absence of graphite clusters in the film structure.

## 5. Conclusions

Electron microscopy of thin carbon films attests unambiguously and Raman spectroscopy indicates indirectly the presence of diamond  $\text{sp}^3$  bonds and to configuration carbon atoms into nanodiamond clusters, whereas the abnormally broadened reflections show strong distortions of interfacial distances  $d(111)$  and  $d(220)$ . At the same time, data of Raman spectroscopy show the presence of  $\text{sp}^2$  bonds in structure of the carbon film. Absence of graphite reflections, that is the absence of pronounced graphite clusters, suggests that hexagonal rings fill the space between diamond clusters and operate as binding elements. This structure is homogeneous and its homogeneity is due to the absence of interfaces.

## Acknowledgements

This work was partly supported by grant 16-05-00873a from the Russian Foundation for Basic Research.

## References

- [1] K.W.R. Gilkes, P.H. Gaskell, J. Robertson, Comparison of neutron scattering data for tetrahedral amorphous-carbon with structural models, *Phys. Rev. B* 51 (N18) (1995) 12303–12312.
- [2] S.D. Berger, D.R. McKenzie, P.J. Martin, EELS analysis of vacuum arc-deposited diamond-like films, *Philos. Mag.* 57 (N6) (1988) 285–290.
- [3] V.N. Inkin, G.G. Kirpilenko, A.A. Dementjev, K.I. Maslakov, A superhard diamond-like carbon film, *Diam. Relat. Mater.* 9 (2000) 715–721.
- [4] S. Xu, B.K. Tay, H.S. Tan, L. Zhong, Y.Q. Tu, S.R.P. Silva, W.I. Milne, Properties of carbon ion deposited tetrahedral amorphous carbon films as a function of ion energy, *J. Appl. Phys.* 79 (N9) (1996) 7234–7240.
- [5] B.K. Tay, D. Sheeja, S.P. Lau, X. Shi, B.C. Seet, Y.C. Yeo, Time and temperature-dependent changes in the structural properties of tetrahedral amorphous carbon films, *Surf. Coat. Technol.* 130 (2000) 248–251.
- [6] V.S. Ostrovsky, Y.S. Virgilyev, V.I. Kostikov, N.N. Shipkov, *Synthetic Graphite*. Moscow, Metalurgiya, (1986), p. 272 (in Russian).
- [7] J. Robertson, E.P. O'Reilly, Electronic and atomic structure of amorphous carbon, *Phys. Rev. B* 35 (N6) (1987) 2946–2957.
- [8] J. Robertson, Diamond-like amorphous carbon, *Mater. Sci. Eng. R* 37 (2002) 129–281.

- [9] B.K. Tay, X. Shi, E.J. Liu, H.S. Tan, L.K. Cheah, Effects of substrate temperature on the properties of tetrahedral amorphous carbon films, *Thin Solid Films* 346 (N1-2) (1999) 155–161.
- [10] A.H. Jayatissa, F. Sato, N. Saito, H. Ohnishi, K. Takizawa, Y. Nakanishi, T. Yamaguchi, Structural properties of carbon films deposited by pulsed ArF laser ablation: effects of substrate temperature, bias and H<sub>2</sub> pressure, *Mater. Sci. Eng. B* 55 (N1–2) (1998) 143–152.
- [11] D.L. Pappas, K.L. Saenger, J. Bruley, W. Krakow, J.J. Cuomo, T. Gu, R.W. Collins, Pulsed laser deposition of diamond-like carbon films, *J. Appl. Phys.* 71 (N11) (1992) 5675–5684.
- [12] S.A. Petrov, About mechanism of nucleation of wurtzite phase of graphite in films, deposited in vacuum from the laser-erosion plasma, *Bestnik BGU ser.1* (N1) (2012) 43–45 (in Russian).
- [13] V.A. Plotnikov, B.F. Demyanov, K.B. Solomatin, S.V. Makarov, V.I. Yarzev, Atomic structure of carbon nanofilms obtained by condensation from the vapor phase. *Fundamental problems of modern material science*, 10 (N1) (2013) 50–55 (in Russian).
- [14] M.D. Starostenkov, I.V. Loschina, B.F. Demyanov, Study of carbon nanostructures using the Tersoff potential. *Fundamental problems of modern material science*, 2 (N1) (2005) 62–67 (in Russian).
- [15] A. Hoffman, A. Heiman, H.P. Strunk, S.H. Christiansen, Microstructure and phase composition evolution of nano-crystalline carbon films: dependence on deposition temperature, *J. Appl. Phys.* 91 (N5) (2002) 3336–3344.
- [16] V.A. Plotnikov, B.F. Demyanov, S.V. Makarov, Effect of intermetallic compounds synthesis on processes of growth and consolidation of detonation nanodiamond nanocrystals, *Pis'ma v ZhTF* 35 (N20) (2009) 10–18 (in Russian).
- [17] M.G. Beghi, A.C. Ferrari, K.B.K. Teo, J. Robertson, C.E. Bottani, A. Libassi, B.K. Tanner, Bonding and mechanical properties of ultrathin diamond-like carbon films, *Appl. Phys. Lett.* 81 (N20) (2002) 3804–3806.
- [18] N. Dwivedi, S. Kumar, H.K. Malik, Superhard behaviour, low residual stress, and unique structure in diamond-like carbon films by simple bilayer approach, *J. Appl. Phys.* 112 (2012) 023518.
- [19] S. Bhargava, H.D. Bist, S. Sahli, M. Aslam, H.B. Tripathi, Diamond polytypes in the chemical vapor deposited diamond films, *Appl. Phys. Lett.* 67 (1995) 1706–1709.
- [20] F. Tuinstra, J.L. Koenig, Raman spectrum of graphite, *J. Chem. Phys.* 53 (1970) 1126–1130.
- [21] A.M. Zaitsev, *Optical Properties of Diamond*, Data Handbook, Springer, Berlin, 2001.
- [22] J.R. Hardy, S.D. Smith, Two-phonon IR lattice absorption in diamond, *Philos. Mag.* (N6) (1961) 1163–1172.
- [23] R. Ramamurti, V. Shanov, R.N. Singh, S. Mamedov, P. Boolchand, Raman spectroscopy study of the influence of processing conditions on the structure of polycrystalline diamond films, *J. Vac. Sci. Technol. A* 24 (N2) (2009) 179–189.
- [24] E.A. Belenkov, E.A. Karnaukhov, Effect of crystal size on interatomic distances in dispersed carbon, *Phys. Solid State* 41 (N4) (1999) 744–747.